Imaging of Rayleigh damping properties of the in vivo brain using parametric Magnetic Resonance Elastography (MRE)

A. Petrov, P.D. Docherty, M. Sellier, J.G. Chase

Department of Mechanical Engineering, University of Canterbury, Christchurch, New Zealand

Motivation

Doctors use manual touch (palpation) to detect malignancy within the tissues

The method is limited to the tissues and organs located in the vicinity of the body surface

Some organs such as heart, liver and brain are not accessible to palpation

Motivation

The stiffness of biological tissue can vary up to two orders of magnitude.Also, depending of physiological state stiffness can vary (muscles)

The cancerous tissue can differ from the surrounding healthy tissue by 2 to 20 fold. So, stiffness is a good diagnostic indicator of the diseases and pathology

None of the gold-standard imaging technologies (CT, MRI or PET) can directly assess tissue elasticity of the tissue which would be extremely useful when planning surgical procedures

Goal:

We want to palpate the brain

↓

Preferably non-invasively

Challenges with the Brain

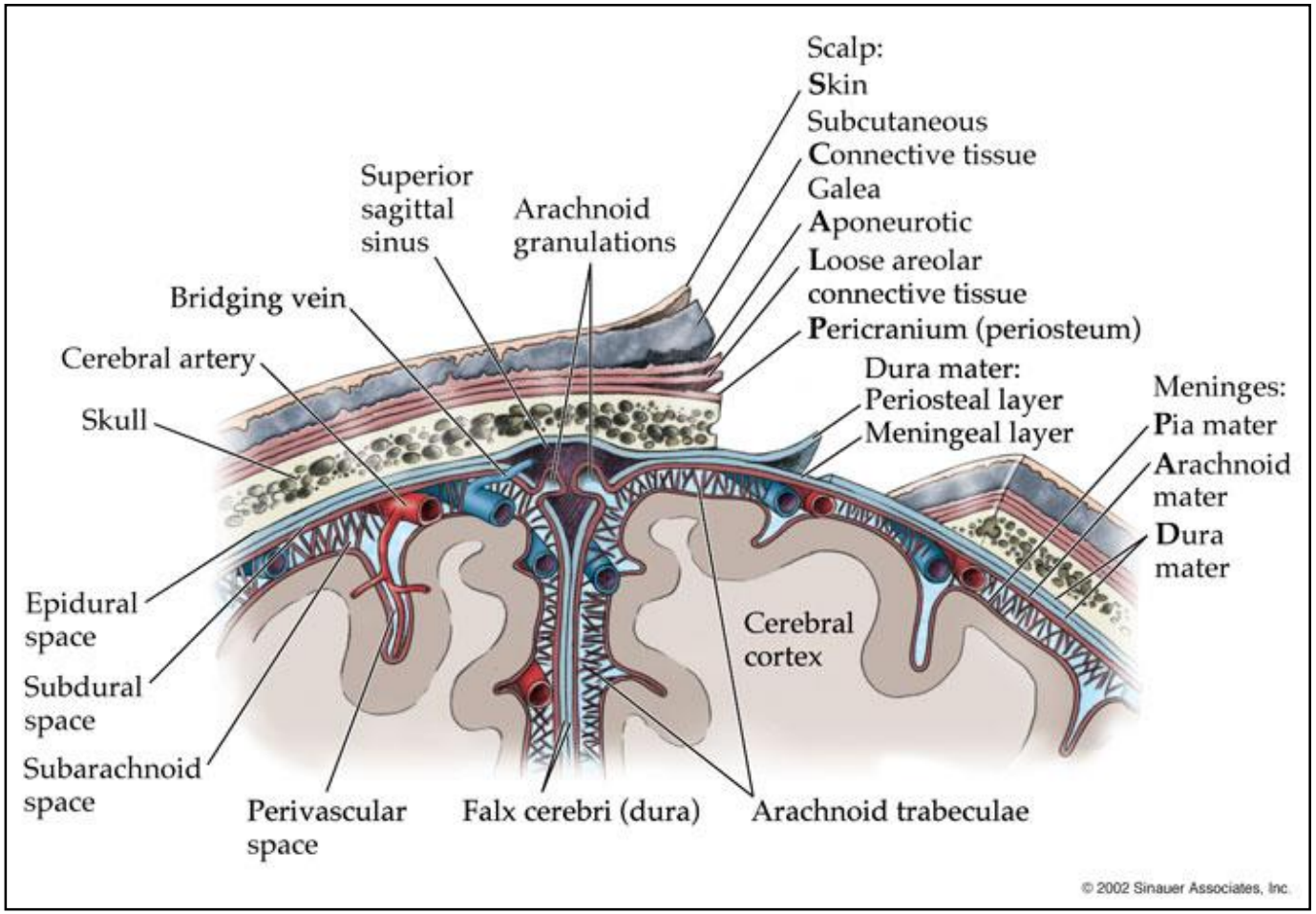

Challenges with the Brain

Elasticity measurement of the brain across different experimental protocols

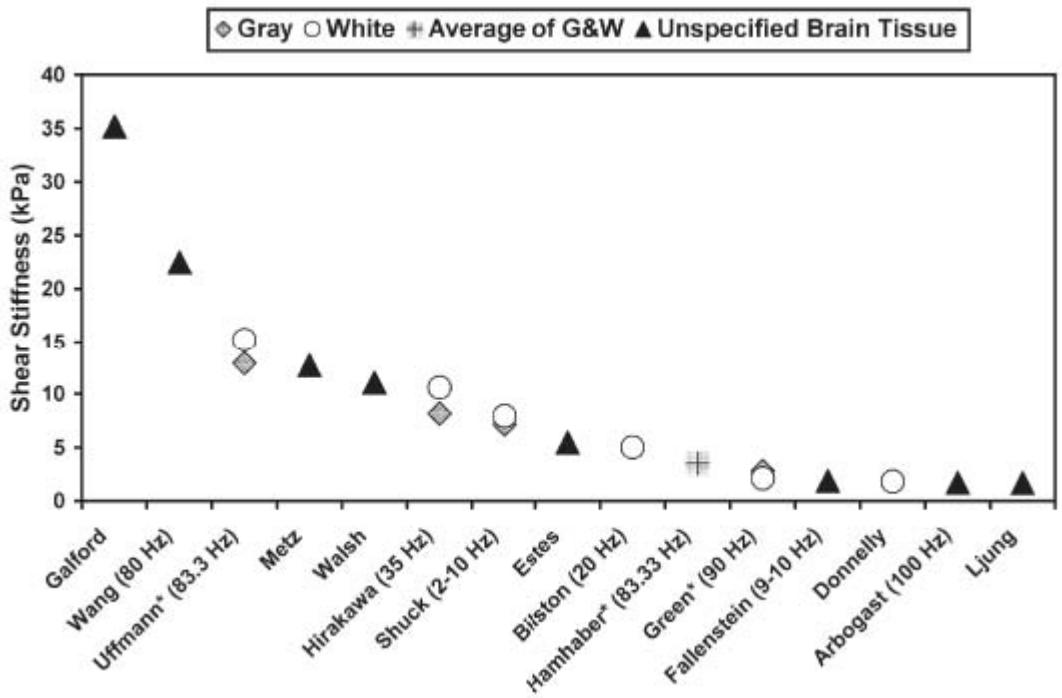

Elasticity imaging overview

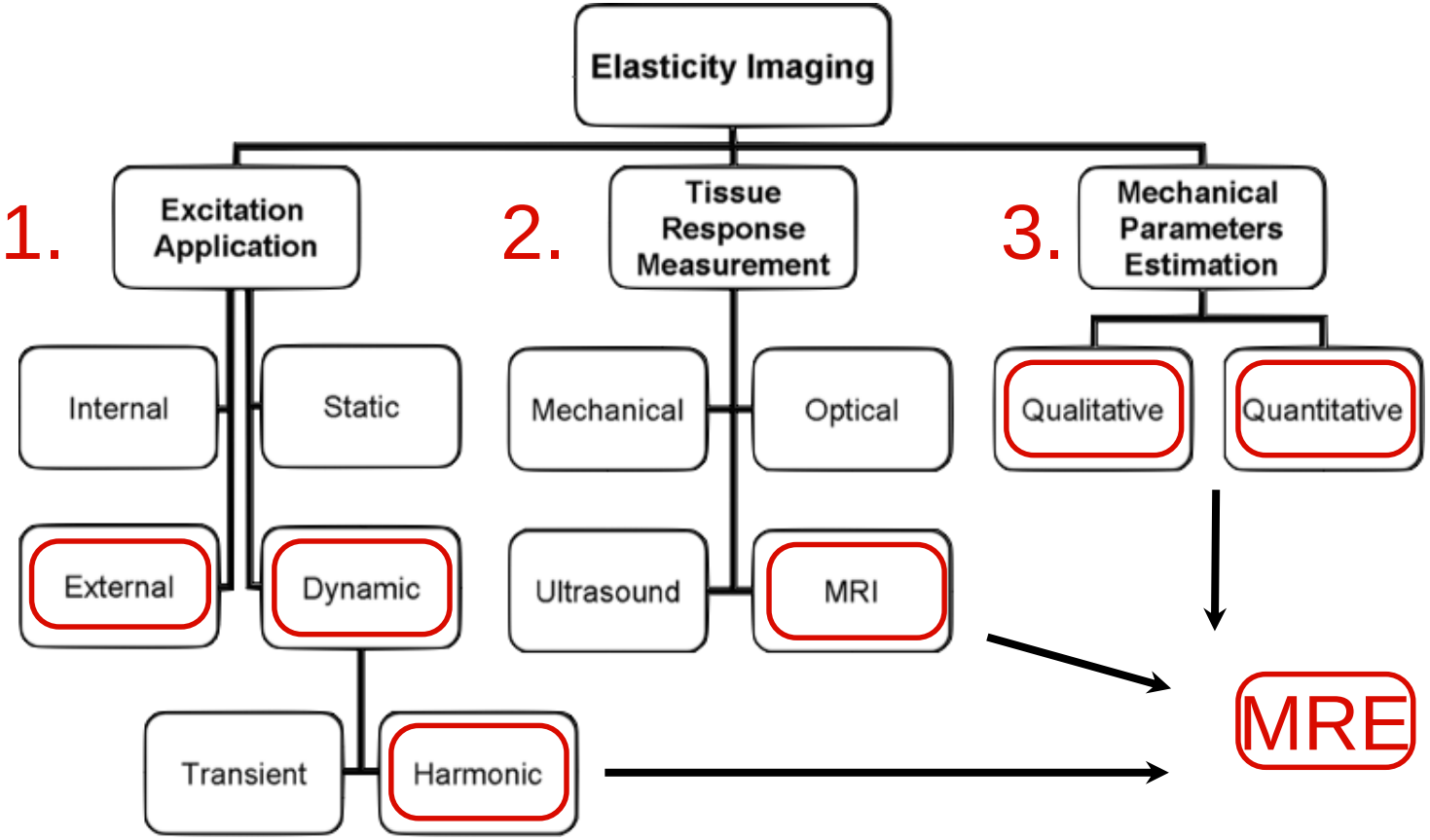

MR Elastography

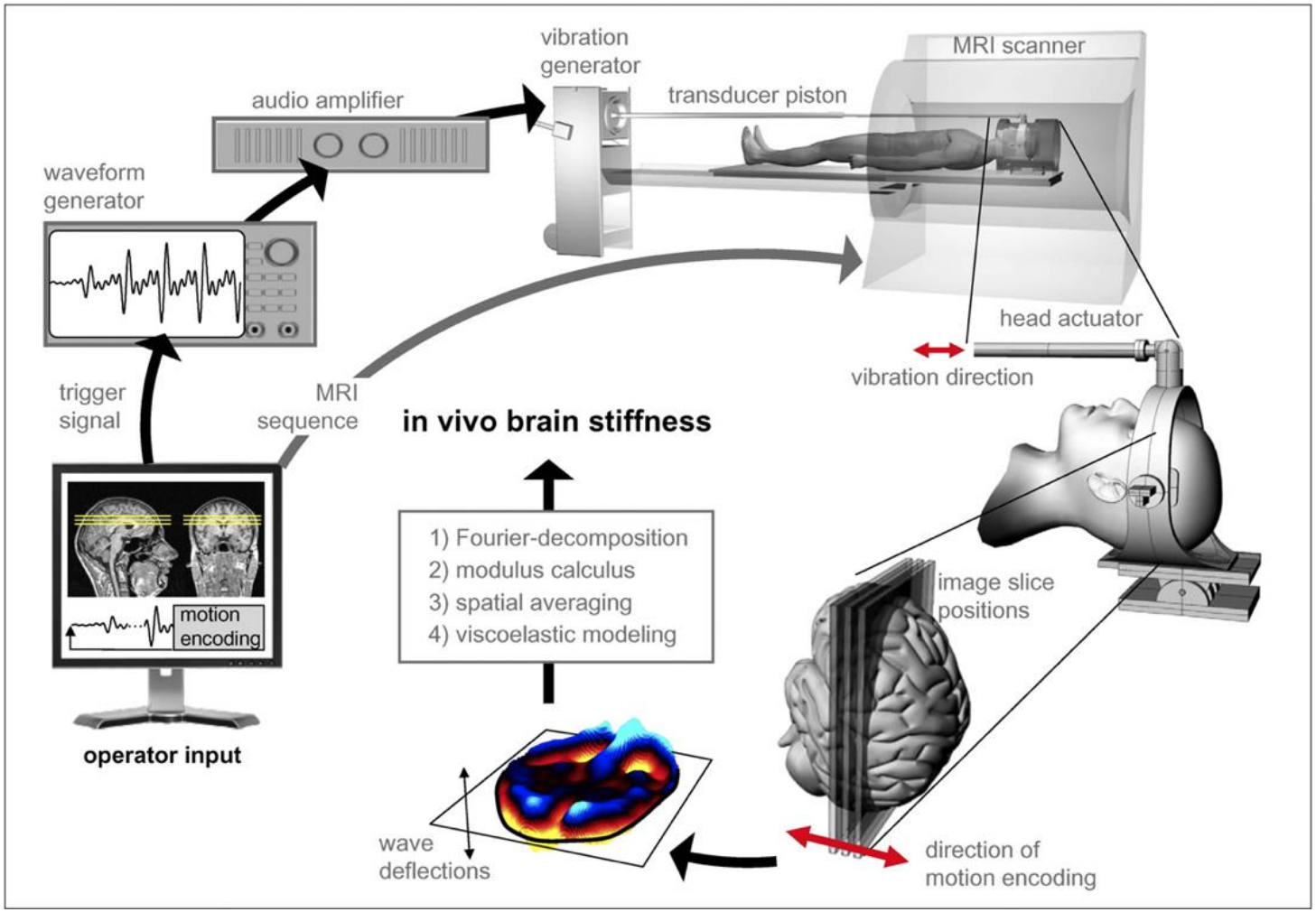

MR Elastography

Head rocker

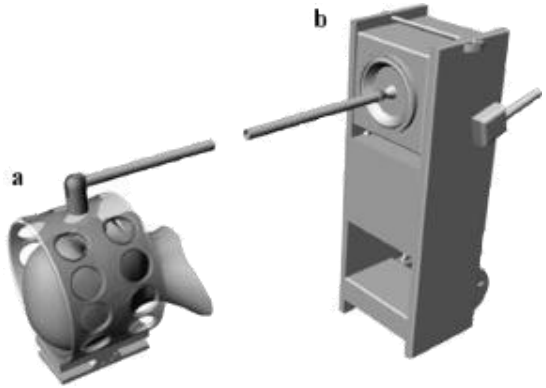

Bite bar

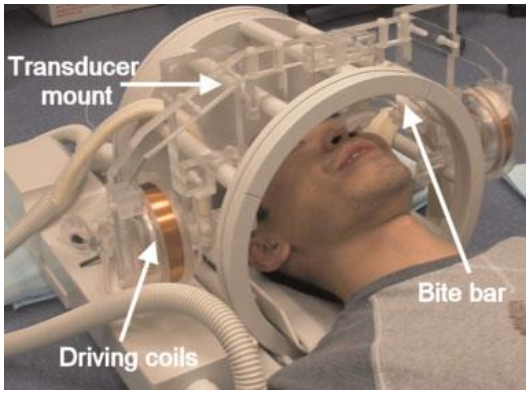

Acoustic

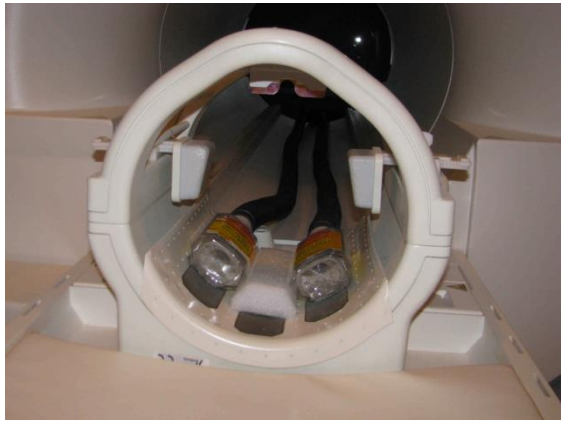

MR Elastography

Motion Encoding

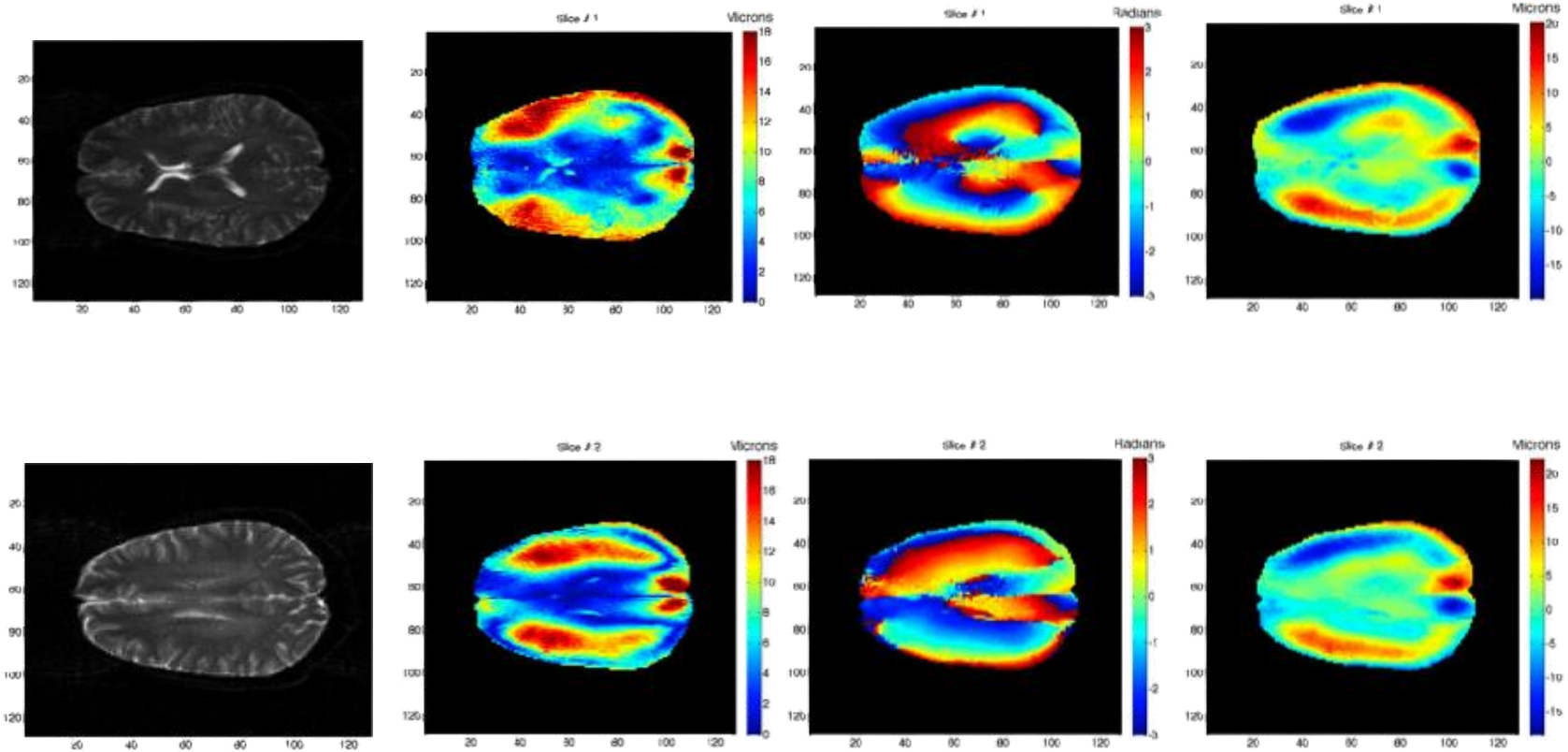

MR-image | Phase | Amplitude | Displacement

Models used in MRE

- Linear / non-linear elastic model
- Linear / non-linear Viscoelastic model
- Poroelastic model
- Rayleigh damping model

Rayleigh damping model

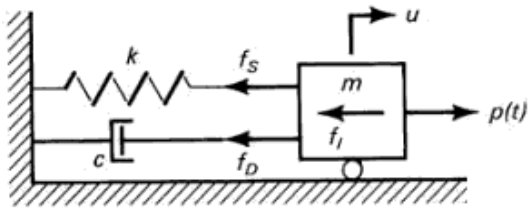

(a)

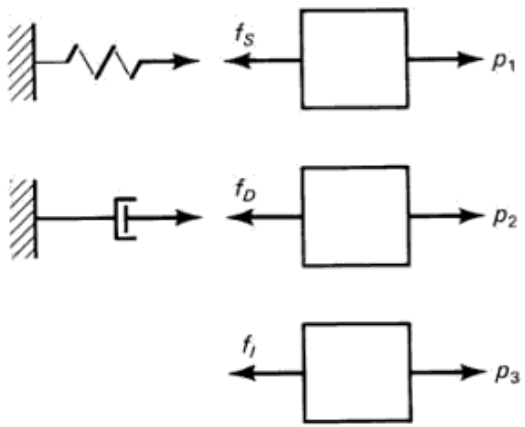

(b)

$$f_S = ku;$$

$$f_D = c\dot{u};$$

$$f_I = m\ddot{u};$$

$$f_I + f_D + f_S = p(t);$$

$$\downarrow$$

$$m\ddot{u} + c\dot{u} + ku = p(t);$$

Rayleigh damping model

$$\mathbf{M}\ddot{\mathbf{u}} + \mathbf{C}\dot{\mathbf{u}} + \mathbf{K}\mathbf{u} = \mathbf{f_t}$$

Time-harmonic steady state

$$\mathbf{u}(\mathbf{x}, t) = \hat{\mathbf{u}}e^{i\omega t}$$
$$\mathbf{f}(\mathbf{x}, t) = \hat{\mathbf{f}}e^{i\omega t}$$

$$\left[-\omega^2\mathbf{M} + i\omega\mathbf{C} + \mathbf{K}\right]\hat{\mathbf{u}} = \hat{\mathbf{f}}.$$

Rayleigh damping assumption

$$\mathbf{C} = \alpha\mathbf{M} + \beta\mathbf{K}.$$

$$\left[-\omega^2\mathbf{M} + i\omega(\alpha\mathbf{M} + \beta\mathbf{K}) + \mathbf{K}\right]\hat{\mathbf{u}} = \hat{\mathbf{f}}.$$

$$\left[-\omega^2\left(1 - \frac{i\alpha}{\omega}\right)\mathbf{M} + (1 + i\omega\beta)\,\mathbf{K}\right]\hat{\mathbf{u}} = \hat{\mathbf{f}},$$

$$\left[-\omega^2\left(\rho - \frac{i\alpha\rho}{\omega}\right)\hat{\mathbf{M}} + (\mu + i\omega\beta\mu)\,\hat{\mathbf{K}}\right]\hat{\mathbf{u}} = \hat{\mathbf{f}},$$

Complexed valued

$$\rho = \rho_R + i\rho_I$$
$$\mu = \mu_R + i\mu_I$$

Rayleigh damping model

$$\rho_R = \rho, \quad \text{and} \quad \rho_I = \frac{-\alpha\rho}{\omega}$$

$$\mu_R = \mu, \quad \text{and} \quad \mu_I = \omega\beta\mu.$$

$$\left[-\omega^2\rho\hat{\mathbf{M}} + \mu\hat{\mathbf{K}}\right]\hat{\mathbf{u}} = \hat{\mathbf{f}},$$

$$\xi_d = \frac{1}{2}\left(\frac{\alpha}{\omega} + \beta\omega\right),$$

$$\xi_d = \frac{1}{2}\left(\frac{\mu_I}{\mu_R} - \frac{\rho_I}{\rho_R}\right).$$

Two-element RD model representation

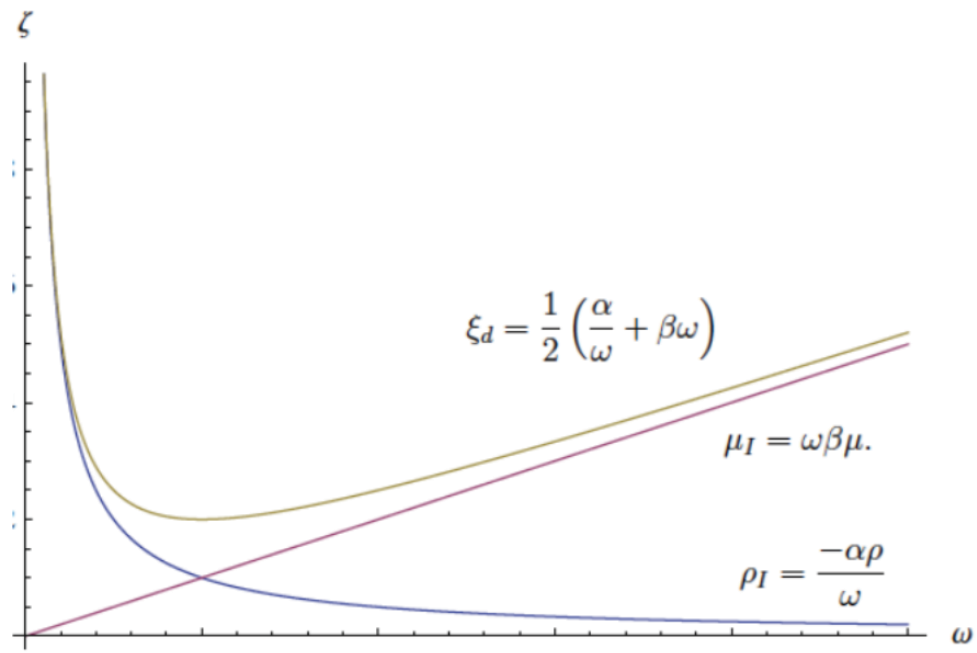

Image reconstruction algorithm

Forward problem

The solution of the FP produces a displacement field by solving the system of PDE using an isotropic RD model

Implemented though Finite Elements (FEA)

Isotropic linear RD model

$$\nabla \cdot (\mu(\nabla \mathbf{u} + \nabla \mathbf{u}^T)) + \nabla(\lambda \nabla \cdot \mathbf{u}) = -\rho\omega^2 \mathbf{u};$$

$$\nabla \cdot (\mu(\nabla \mathbf{u} + \nabla \mathbf{u}^T)) - \nabla(\frac{1}{3}\nabla \cdot \mathbf{u}) - \nabla P = -\rho\omega$$

$$\nabla P = K \nabla \cdot \mathbf{u} = K\left(\frac{\partial u_x}{\partial x} + \frac{\partial u_y}{\partial y} + \frac{\partial u_z}{\partial z}\right);$$

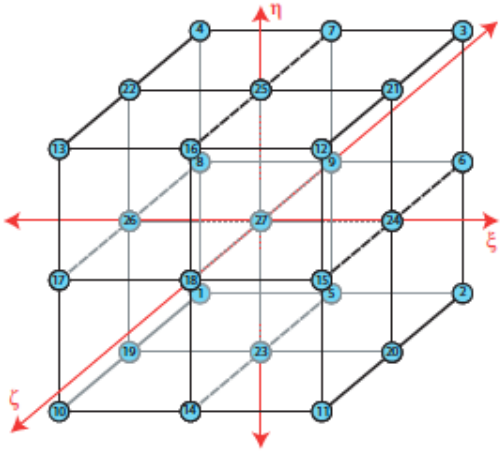

Image reconstruction algorithm

Finding the material property distribution, θ given the mechanical response with respect to the applied boundary conditions.

The inverse problem is implemented through the use of nonlinear optimization-based techniques (CG, GN), which involves finding the θ that minimizes an objective error function:

$$\boldsymbol{\theta} = \arg\min_{\boldsymbol{\theta}}[\boldsymbol{\Phi}],$$

where $\boldsymbol{\Phi}$ is further minimized by the nonlinear iteration process

$$\Phi(\boldsymbol{\theta}) = \sum_{i=1}^{N_m} (\mathbf{u}_i^m - \mathbf{u}_i^c(\boldsymbol{\theta}))(\mathbf{u}_i^m - \mathbf{u}_i^c(\boldsymbol{\theta}))^H,$$

Image reconstruction algorithm

Subzone concept

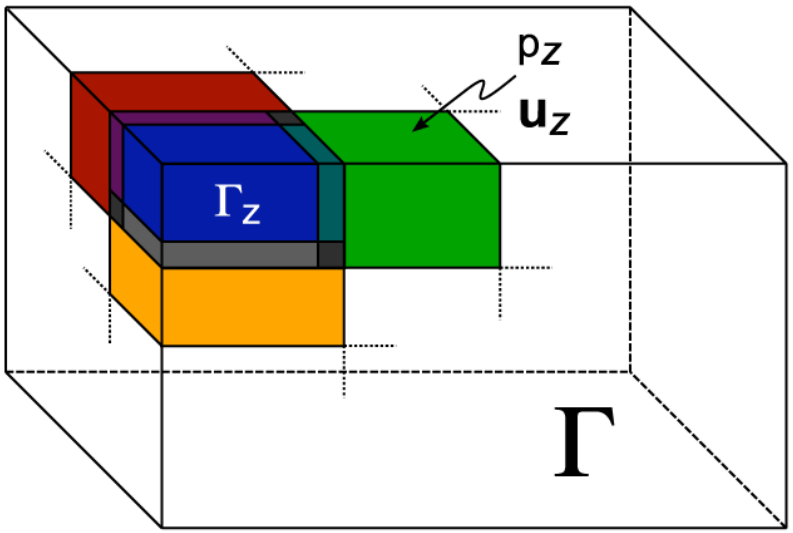

Number of overlapping subzones

Minimization is performed on each subzone

$$\min \mathbf{F}_\Omega(\boldsymbol{\theta}_\Omega) = \min \left\{ \sum_{z=1}^{N_z} \mathbf{F}_z(\boldsymbol{\theta}_z) \right\} = \sum_{z=1}^{N_z} \min \mathbf{F}_z(\boldsymbol{\theta}_z),$$

Initial RD simulation studies

However, when the contributions of damping are Identified in concert, there is a non-identifiability

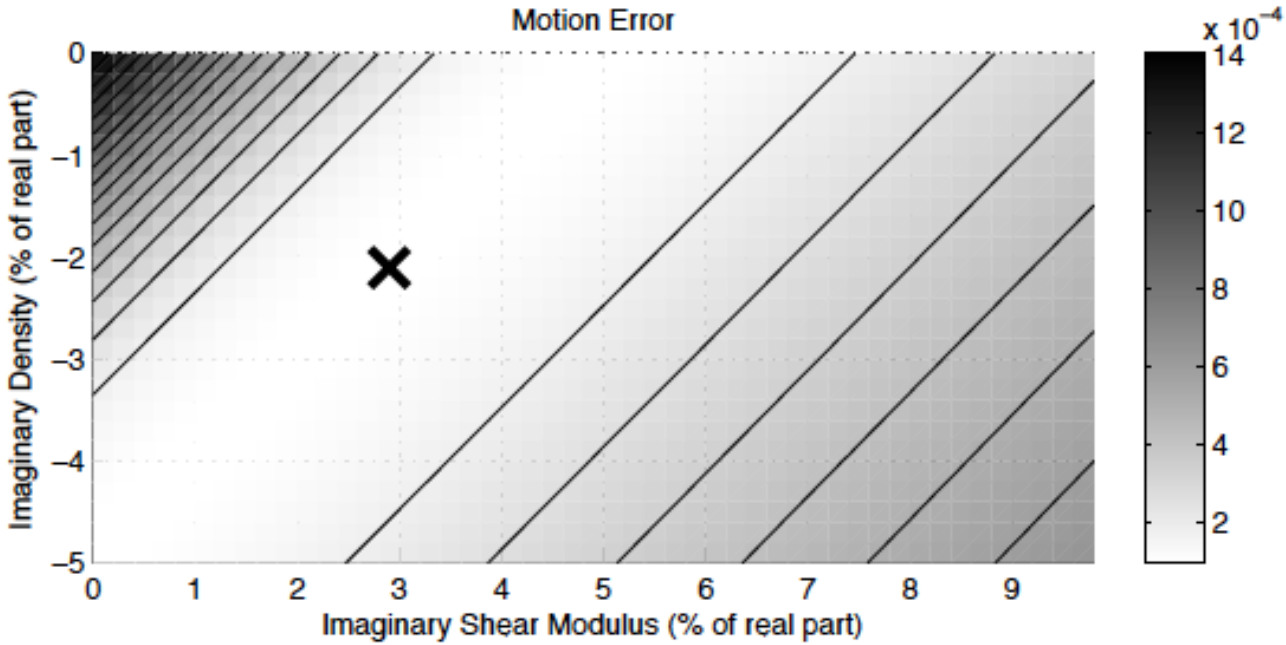

RD phantom experiment

A number of experiments were performed on homogeneous and heterogeneous phantoms to evaluate the RD model

Lightly damped gelatin phantoms

Tofu-Gelatin damping phantoms

Tofu-fluid damping phantom (simplified brain model)

Porous structure of the tofu is a good approximation for brain tissue

RD phantom experiment

Phantom configuration and actuation methodology

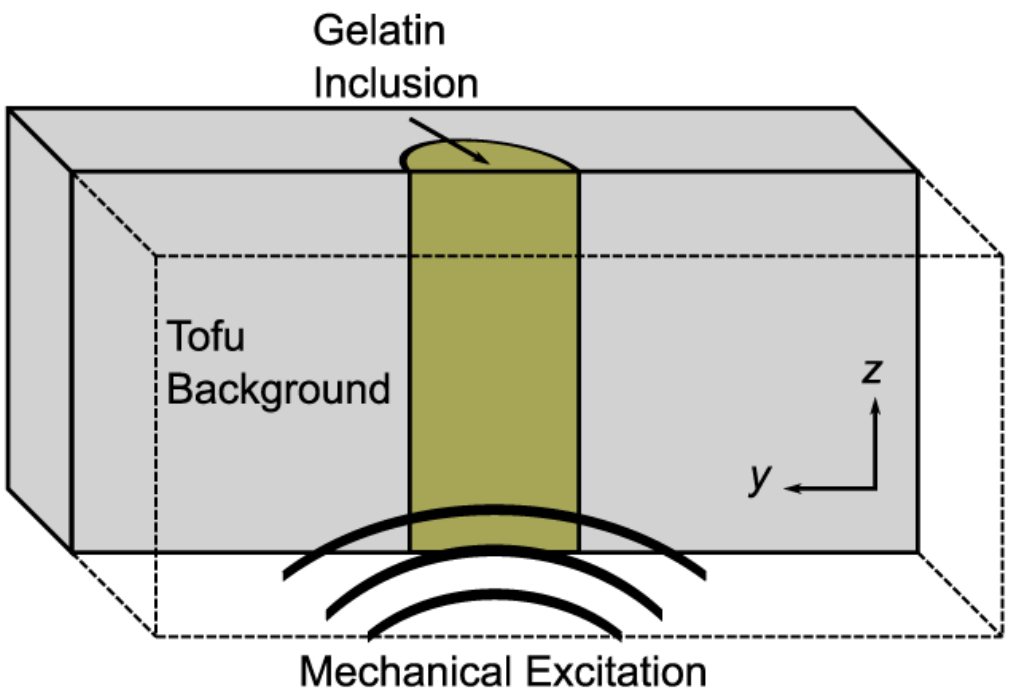

RD phantom experiment

Re shear modulus (Pa) | Im shear modulus (Pa) | Im density (kg/m^3) | Damping ratio (%)

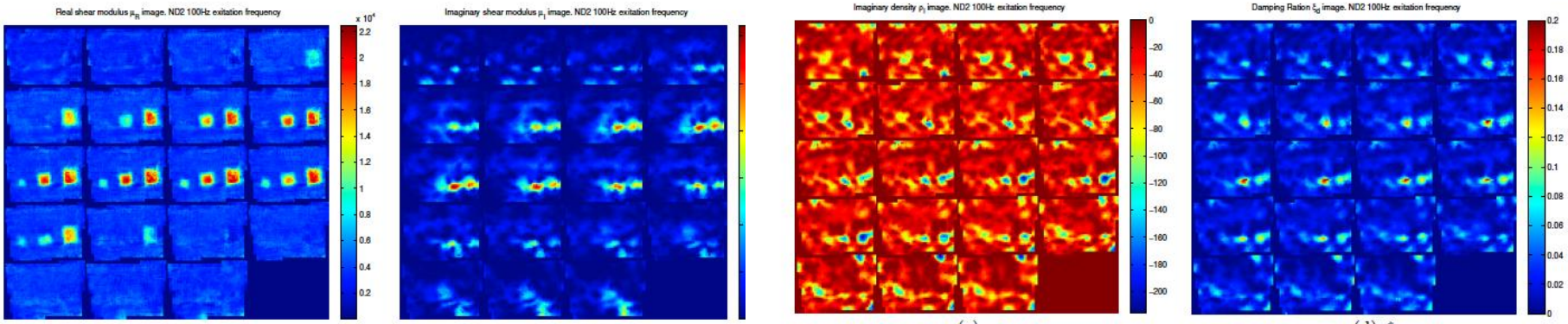

(a) μ_R (b) μ_I (c) ρ_I (d) ξ_d

Parameter Units	μ_R (Pa)	μ_I (Pa)	ρ_I (kg/m^3)	ξ_d (% / 100)
	Median [IQR]	Median [IQR]	Median [IQR]	Median [IQR]
Background (Agar gel 1 %)	3837 [3476 – 4213]	31[14 – 57]	–21 [-38 – -10]	0.016 [0.0097 – 0.026]
Inclusions (Agar gel 2 %)	11571 [9154 – 15180]	61 [30 – 86]	-7 [-26 – -3]	0.006 [0.003 – 0.017]

RD phantom experiment

Re shear modulus (Pa)

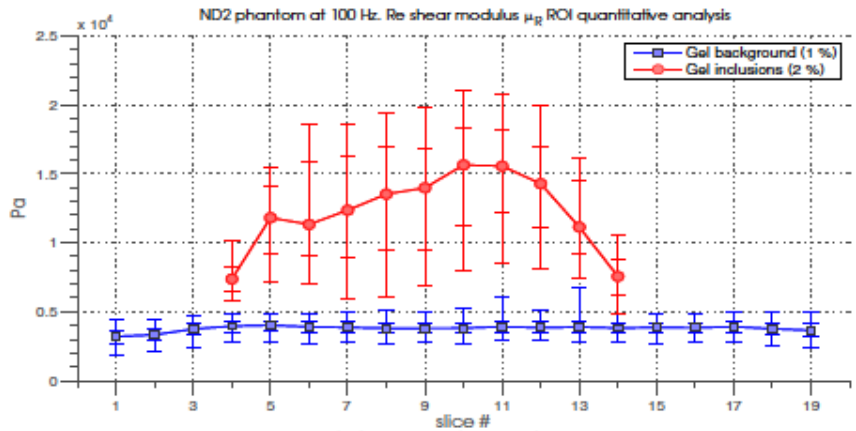

(c) μ_R (ROI)

Im Shear modulus (Pa)

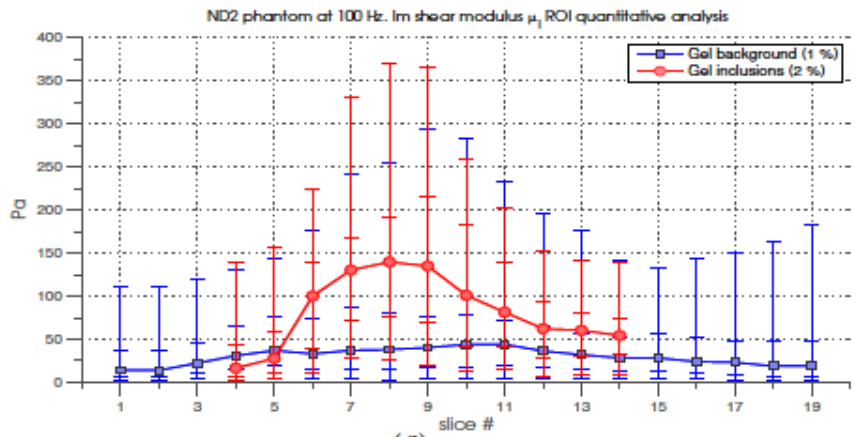

(f) μ_I

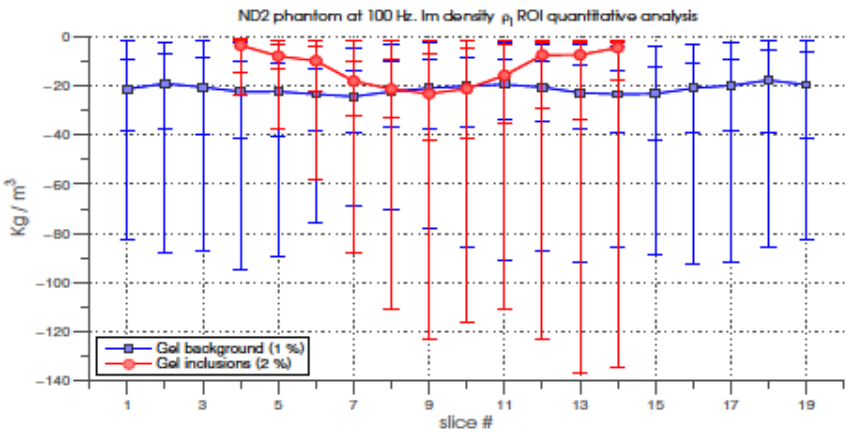

(i) ρ_I (ROI)

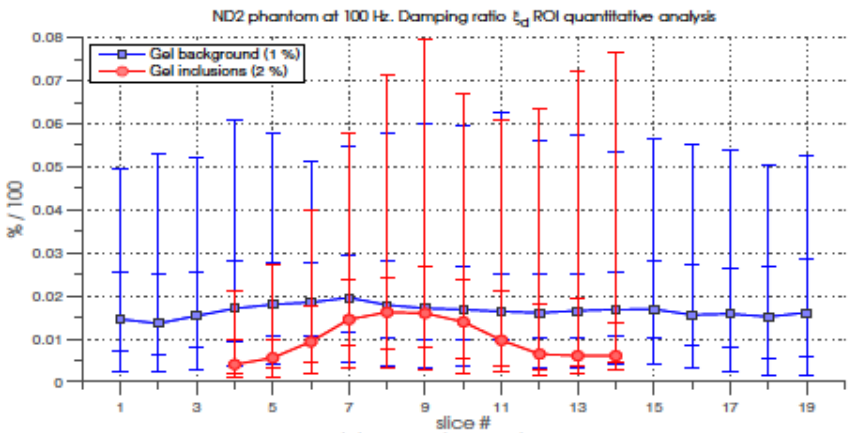

(l) ξ_d (ROI)

RD phantom experiment

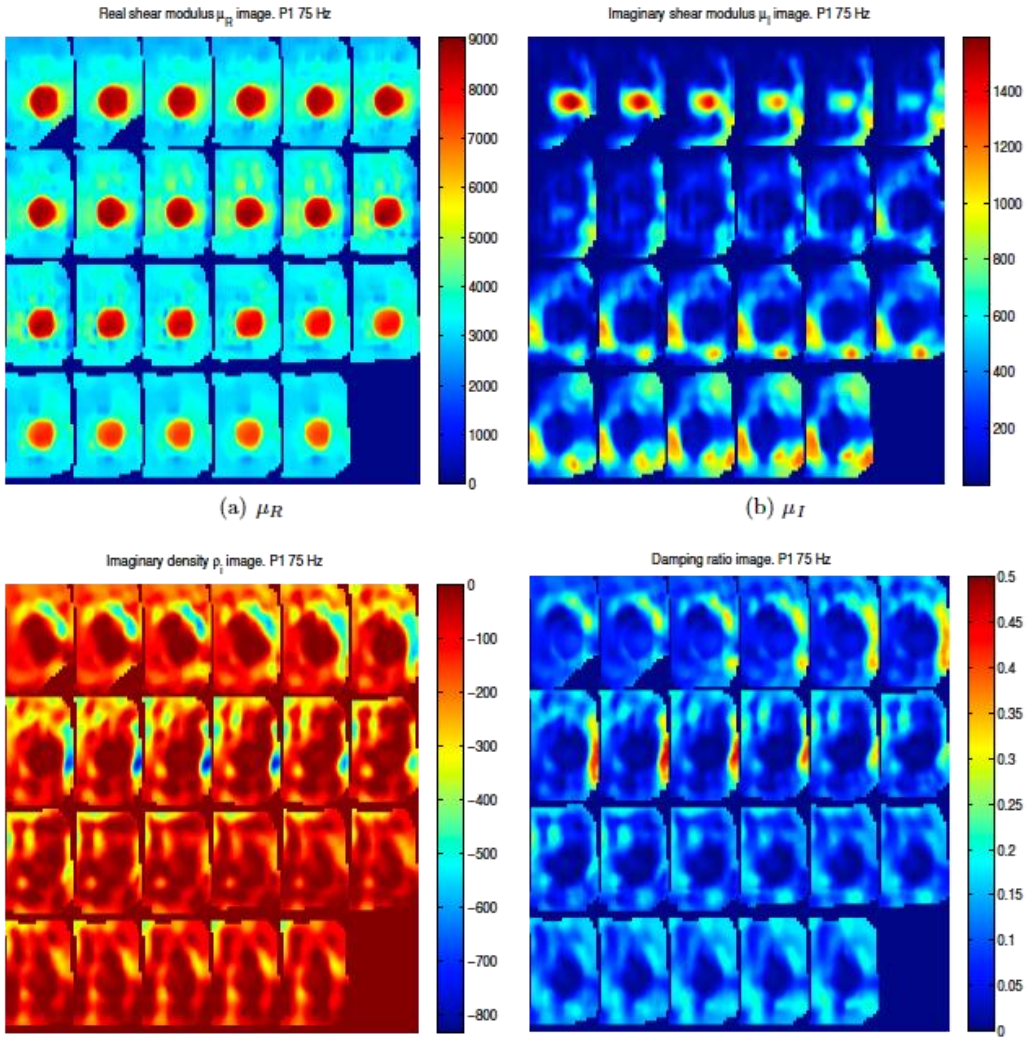

(a) μ_R (b) μ_I

(c) ρ_I (d) ξ

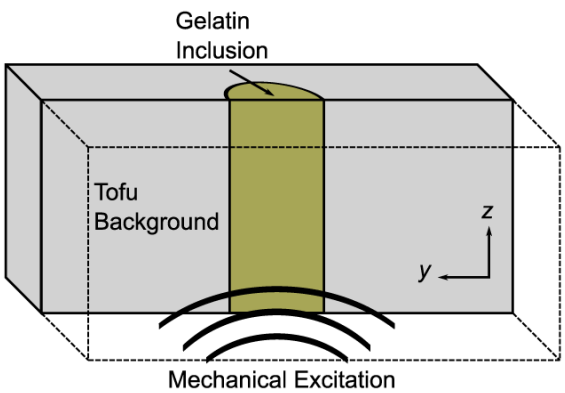

RD phantom experiment

Re shear modulus (Pa)

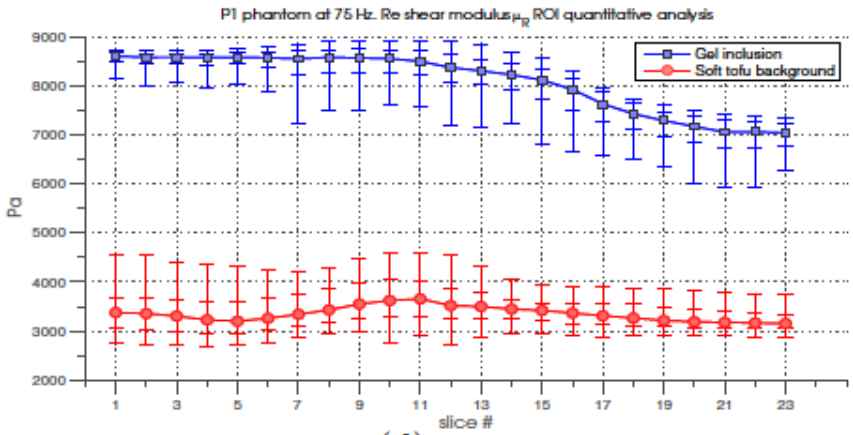

(d) μ_R

Im Shear modulus (Pa)

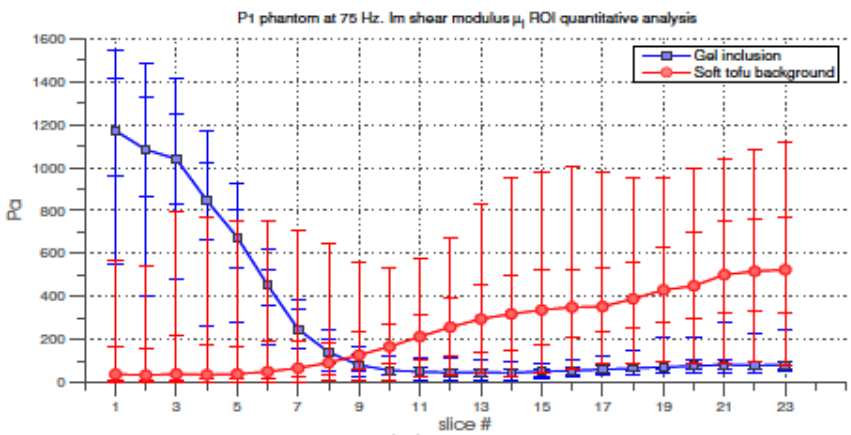

(g) μ_I

Im density (kg/m^3)

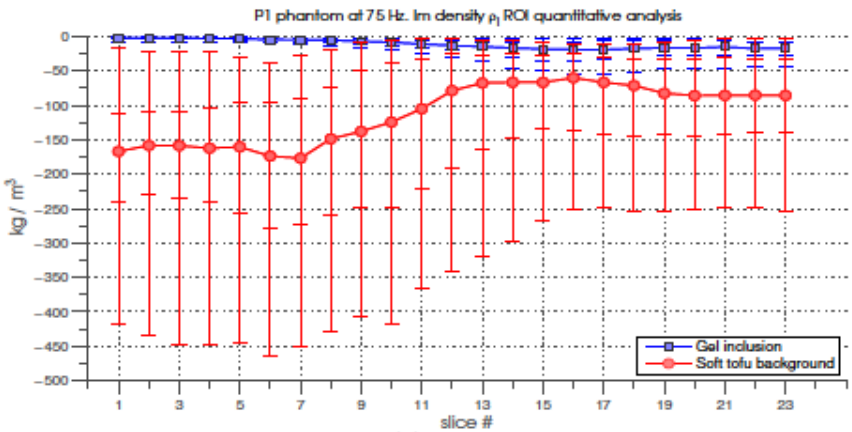

(j) ρ_I

Damping ratio

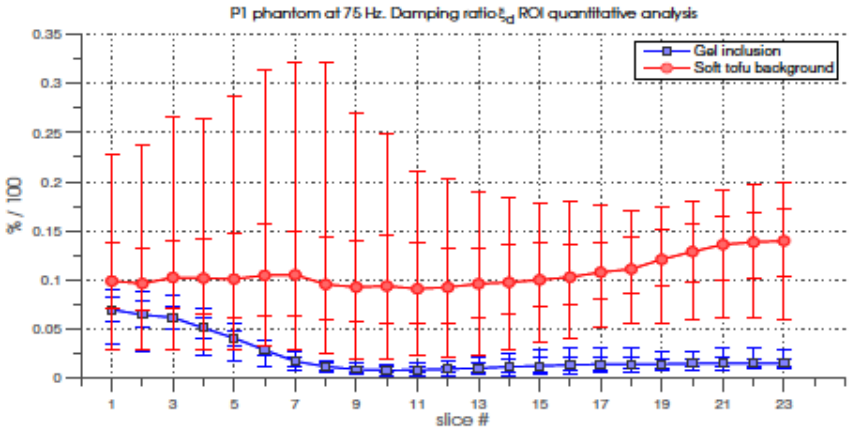

(m) ξ_d

RD phantom experiment

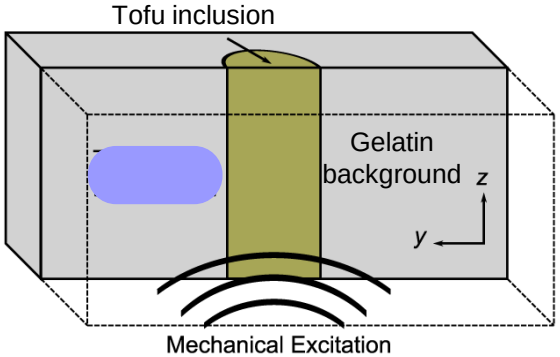

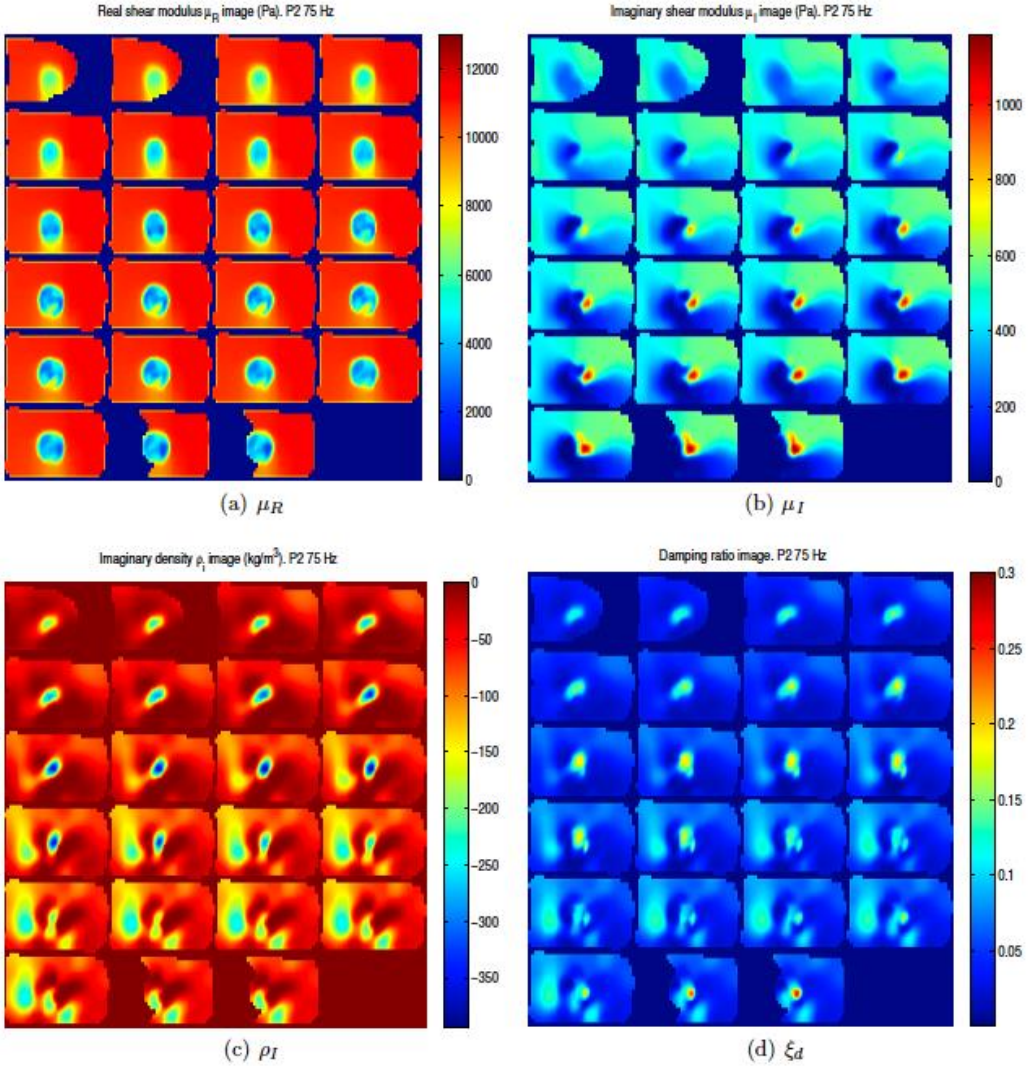

RD phantom experiment

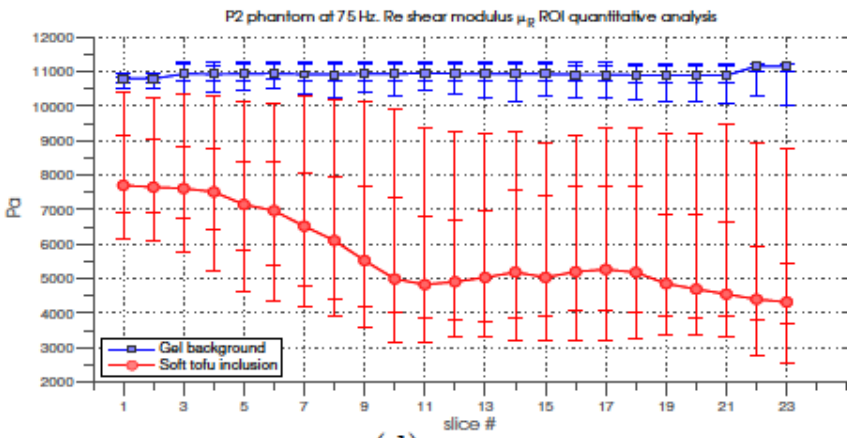

(d) μ_R

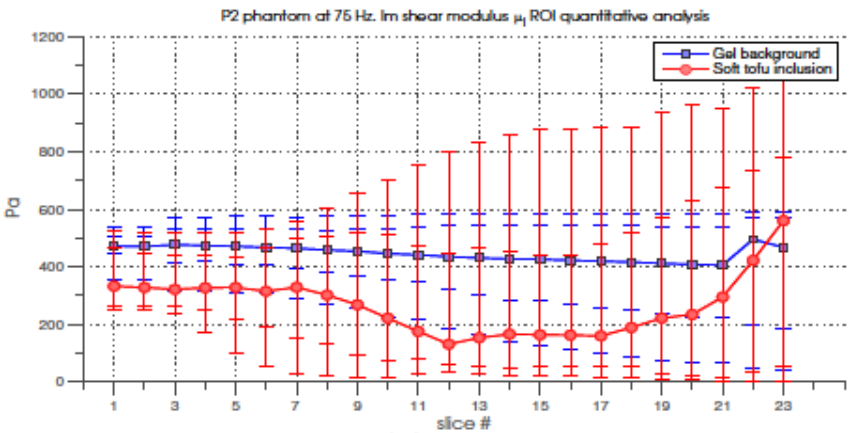

(g) μ_I

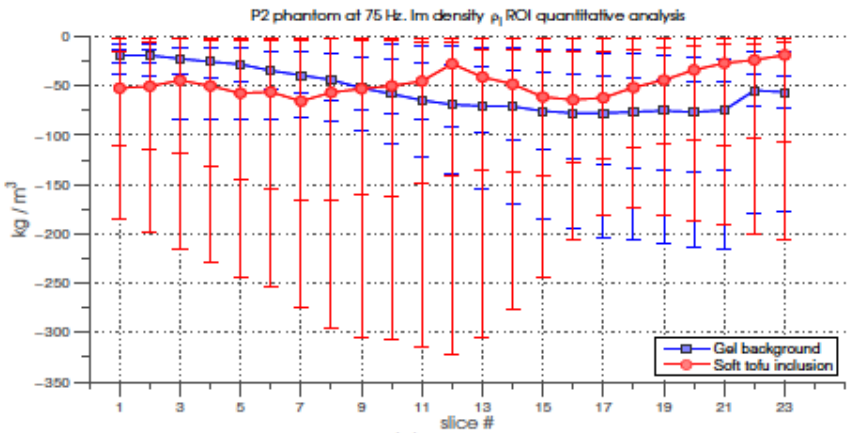

(j) ρ_I

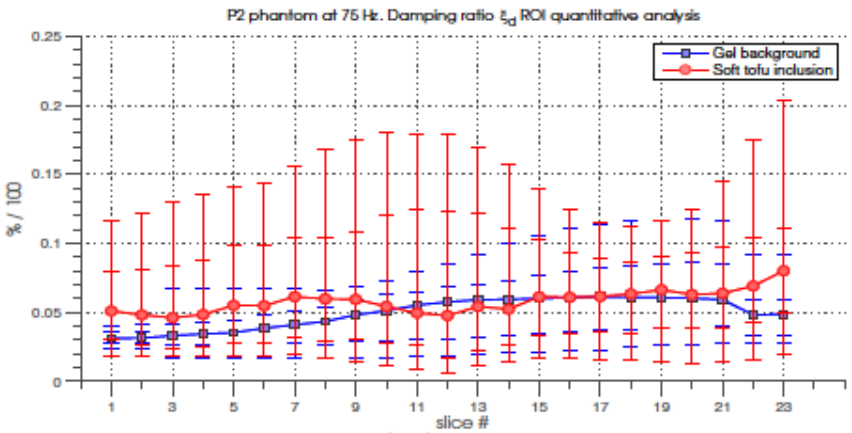

(m) ξ_d

RD phantom experiment

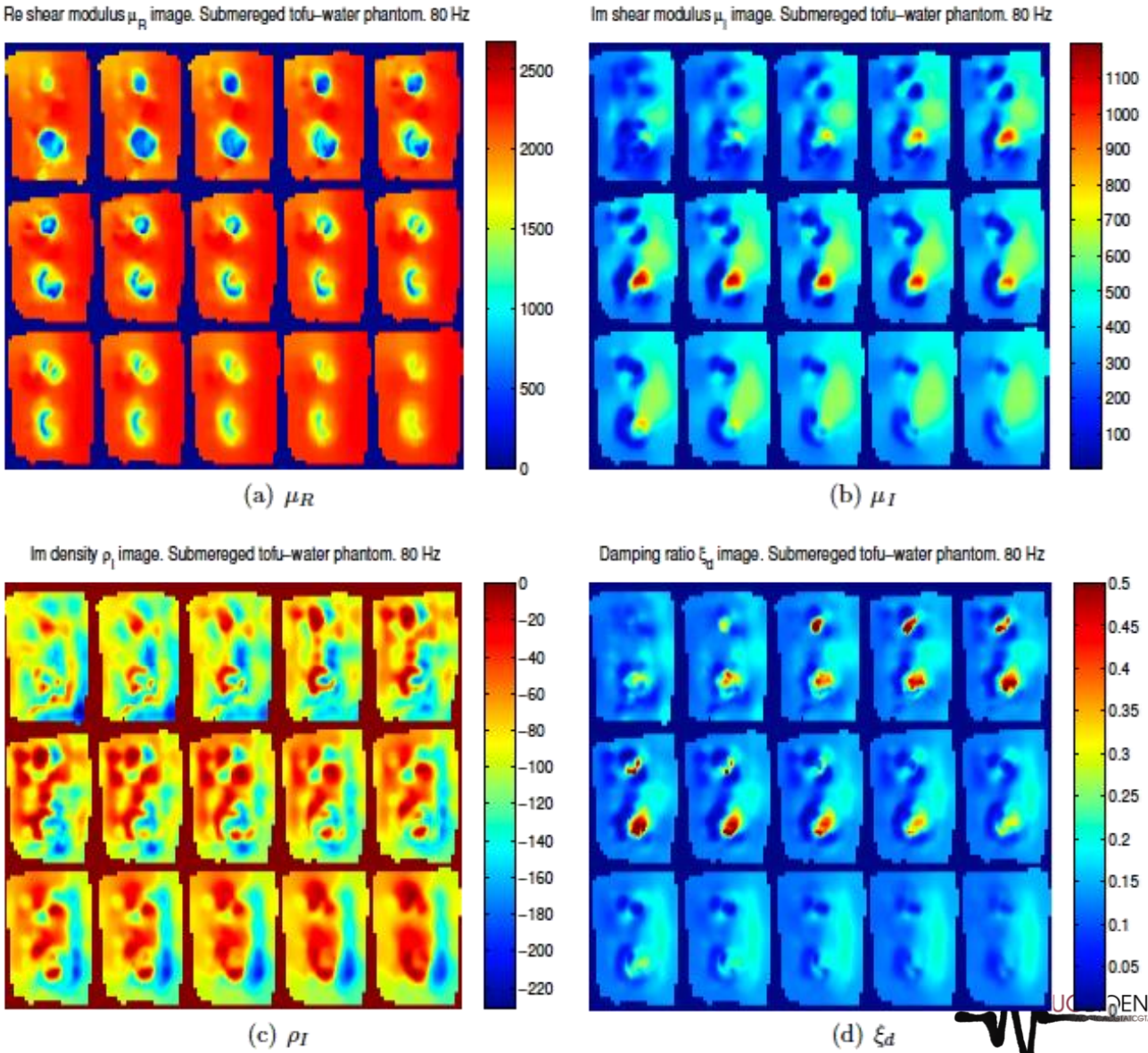

(a) μ_R (b) μ_I

(c) ρ_I (d) ξ_d

Structural analysis

$$\mathbf{M}\ddot{\mathbf{u}} + \mathbf{C}\dot{\mathbf{u}} + \mathbf{K}\mathbf{u} = \mathbf{f_t}$$

Time-harmonic steady state

$$\mathbf{u}(\mathbf{x}, t) = \hat{\mathbf{u}} e^{i\omega t}$$
$$\mathbf{f}(\mathbf{x}, t) = \hat{\mathbf{f}} e^{i\omega t}$$

$$\left[-\omega^2 \mathbf{M} + i\omega \mathbf{C} + \mathbf{K} \right] \hat{\mathbf{u}} = \hat{\mathbf{f}}.$$

Rayleigh damping assumption

$$\mathbf{C} = \alpha \mathbf{M} + \beta \mathbf{K}.$$

$$\left[-\omega^2 \mathbf{M} + i\omega(\alpha \mathbf{M} + \beta \mathbf{K}) + \mathbf{K} \right] \hat{\mathbf{u}} = \hat{\mathbf{f}}.$$

$$\alpha = \frac{-\omega \rho_I}{\rho_R} \qquad \beta = \frac{\mu_I}{\omega \mu_R}.$$

$$\left[-\omega^2 \rho_R + i\omega \left(\frac{-\omega \rho_I}{\rho_R} \rho_R + \frac{\mu_I}{\omega \mu_R} \mu_R \right) + \mu_R \right] \hat{\mathbf{u}} = \hat{\mathbf{f}},$$

$$\left[-\omega^2 \rho_R + i\omega \left(\frac{\mu_I}{\omega} - \omega \rho_I \right) + \mu_R \right] \hat{\mathbf{u}} = \hat{\mathbf{f}}$$

$$\left[-\omega^2 \rho_R + \mu_R \right] \mathbf{u}_R + \left[\mu_I - \omega^2 \rho_I \right] \mathbf{u}_I = \hat{\mathbf{f}}.$$

Structural analysis

$$\left[-\omega^2\rho_R+\mu_R\right]\mathbf{u}_R+\left[\mu_I-\omega^2\rho_I\right]\mathbf{u}_I=\hat{\mathbf{f}}.$$

$$\left[-\omega^2\rho_R+\mu_R\right]\mathbf{u}_R=\hat{\mathbf{f}}_R$$

$$\rho_R=1000\ kg/m^3.$$

known + unknown = known

$$\mu_R=\hat{\mathbf{f}}_R/\mathbf{u}_R+\omega^2\rho_R$$

$$\left[-\omega^2\rho_I+\mu_I\right]\mathbf{u}_I=\hat{\mathbf{f}}_I$$

unknown + unknown = known

Not possible to solve

Solution: multiple frequencies

$$\begin{pmatrix} -\omega_1^2\mathbf{u}_{I1} & \mathbf{u}_{I1} \\ \vdots & \vdots \\ -\omega_2^2\mathbf{u}_{I2} & \mathbf{u}_{I2} \\ \vdots & \vdots \end{pmatrix}\begin{pmatrix}\rho_I \\ \mu_I\end{pmatrix}=\begin{matrix}[1] \\ \\ [5] \\ \\ \end{matrix}\begin{pmatrix}\hat{\mathbf{f}}_{I1} \\ \vdots \\ \hat{\mathbf{f}}_{I2} \\ \vdots\end{pmatrix}$$

$\omega_1 \neq \omega_2.$

Condition for the theoretical identifiability

$\omega_1 \gg \omega_2$ or $\omega_1 \ll \omega_2$

Condition for strong practical identifiability

Structural analysis

Theoretically, but not practically identifiable

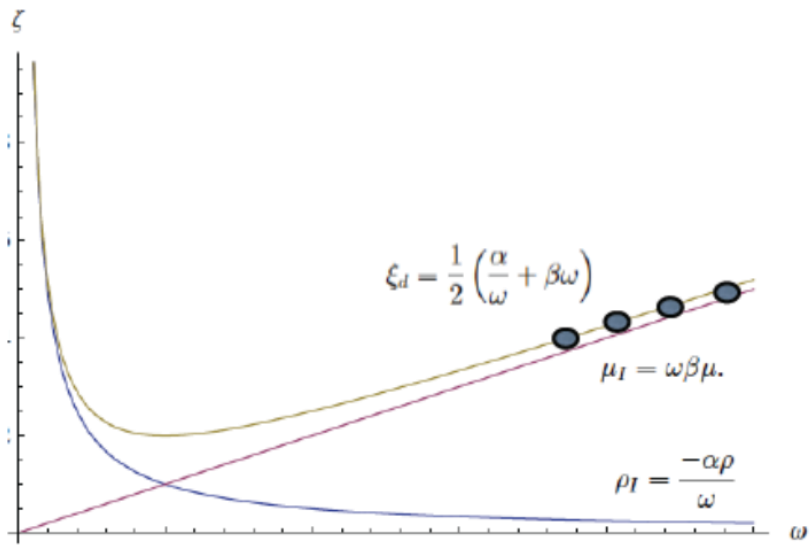

Condition for strong practical identifiability

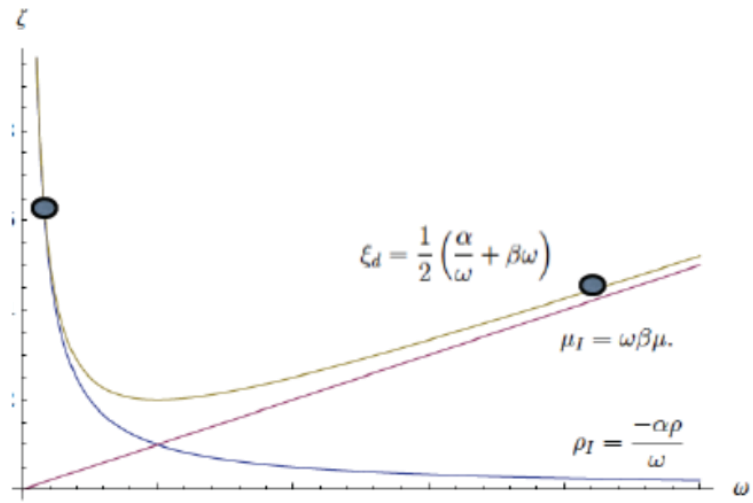

$\omega_1 \approx \omega_2$

$$\begin{pmatrix} -\omega_1^2 \mathbf{u}_{I1} & \mathbf{u}_{I1} \\ \vdots & \vdots \\ -\omega_2^2 \mathbf{u}_{I2} & \mathbf{u}_{I2} \\ \vdots & \vdots \end{pmatrix} \begin{pmatrix} \rho_I \\ \mu_I \end{pmatrix} = \begin{matrix} [1] \\ \\ [5] \\ \\ \end{matrix} \begin{pmatrix} \hat{\mathbf{f}}_{I1} \\ \vdots \\ \hat{\mathbf{f}}_{I2} \\ \vdots \end{pmatrix}$$

$\omega_1 \gg \omega_2$ or $\omega_1 \ll \omega_2$

Structural analysis

$$\left[-\omega^2\rho_R + \mu_R\right]\mathbf{u}_R + \left[\mu_I - \omega^2\rho_I\right]\mathbf{u}_I = \hat{\mathbf{f}}.$$

$$\left[-\omega^2\rho_I + \mu_I\right]\mathbf{u}_I = \hat{\mathbf{f}}_I$$

↓

unknown + unknown = known → Non possible to solve

↓

Solution: parametrization → estimate + unknown = known

$$\begin{pmatrix}\mathbf{u}_I\\ \mathbf{u}_I\\ \vdots\\ \mathbf{u}_I\end{pmatrix}\left(\mu_I\right) = \begin{pmatrix}\hat{\mathbf{f}}_I + \omega^2\rho_I\mathbf{u}_I\\ \hat{\mathbf{f}}_I + \omega^2\rho_I\mathbf{u}_I\\ \vdots\\ \mathbf{f}_I + \omega^2\rho_I\mathbf{u}_I\end{pmatrix}$$

Constraining imaginary density

$$\begin{pmatrix}-\omega^2\mathbf{u}_I\\ -\omega^2\mathbf{u}_I\\ \vdots\\ -\omega^2\mathbf{u}_I\end{pmatrix}\left(\rho_I\right) = \begin{pmatrix}\hat{\mathbf{f}}_I - \mu_I\mathbf{u}_I\\ \hat{\mathbf{f}}_I - \mu_I\mathbf{u}_I\\ \vdots\\ \mathbf{f}_I + \mu_I\mathbf{u}_I\end{pmatrix}$$

Constraining imaginary shear modulus

Structural analysis

- The model has proved to be non-ID
- Two alternative solutions were developed
    1. Simultaneous MF inversion
    2. Parametric inversion

Multifrequency phantom studies

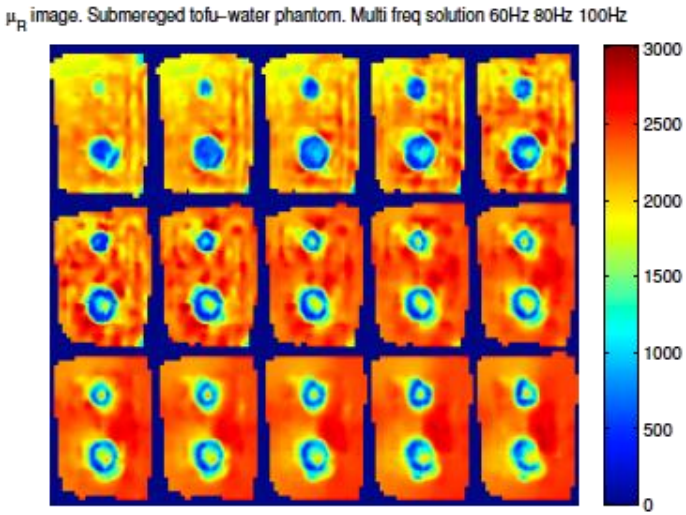

(a) μ_R (MF)

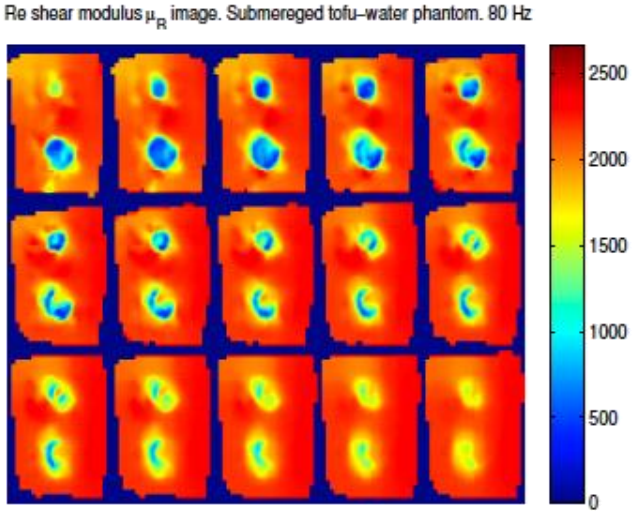

(b) μ_R (SF)

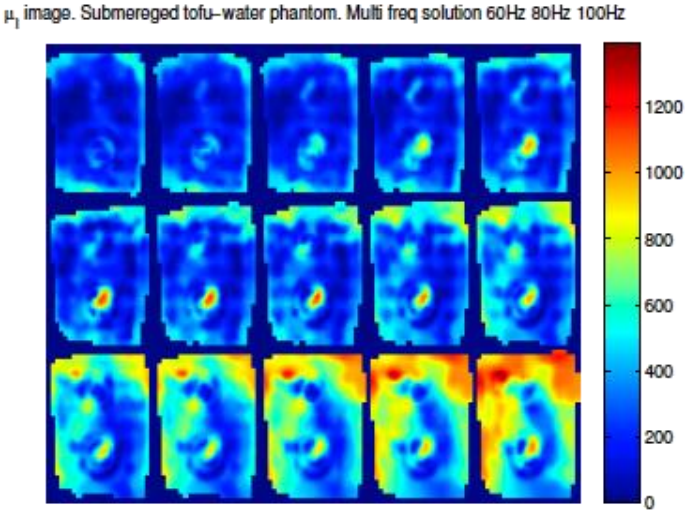

(c) μ_I (MF)

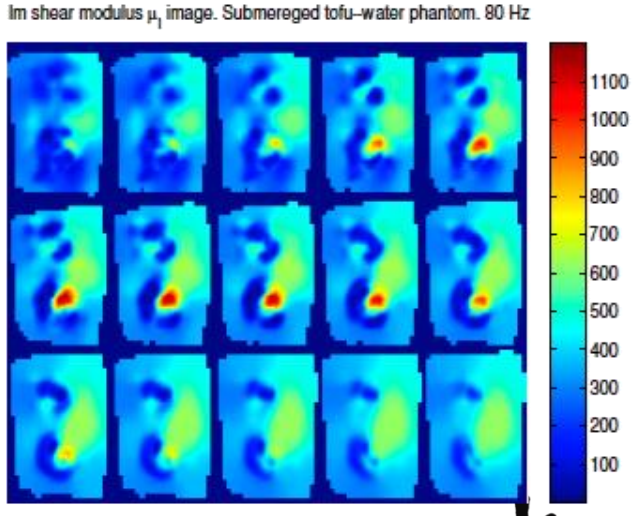

(d) μ_I (SF)

Multifrequency phantom studies

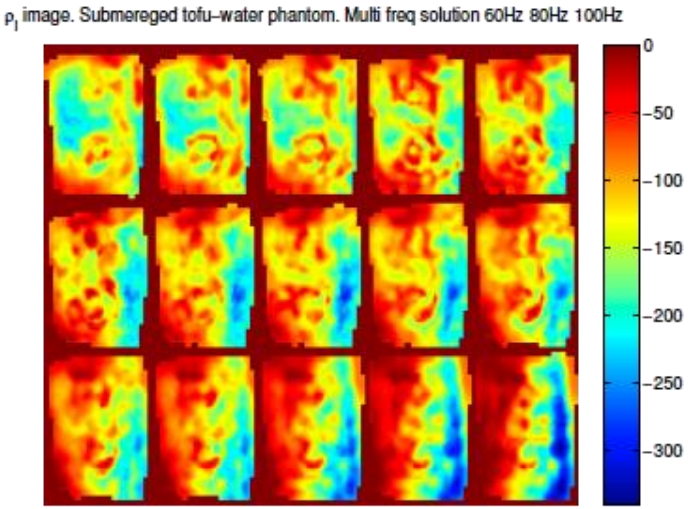

(e) ρ_I (MF)

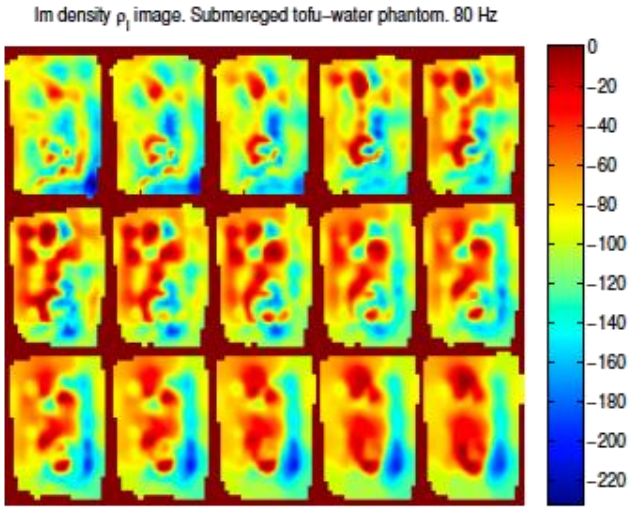

(f) ρ_I (SF)

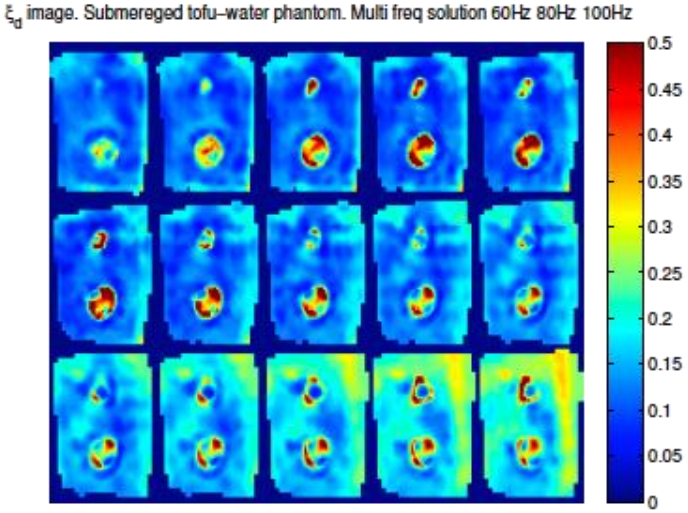

(g) ξ_d (MF)

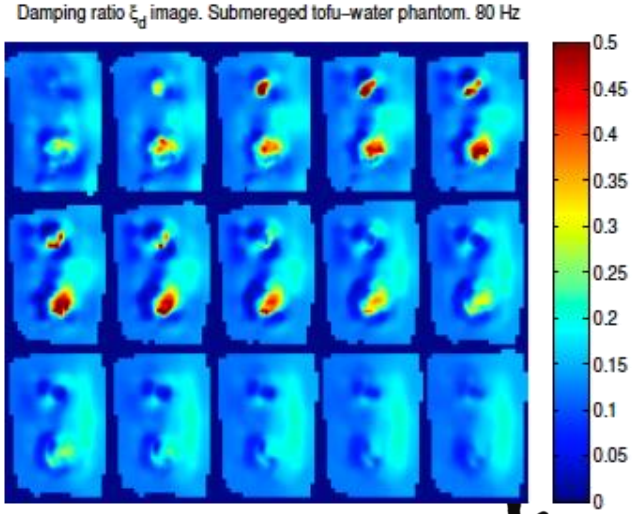

(h) ξ_d (SF)

Parametric RD reconstructions

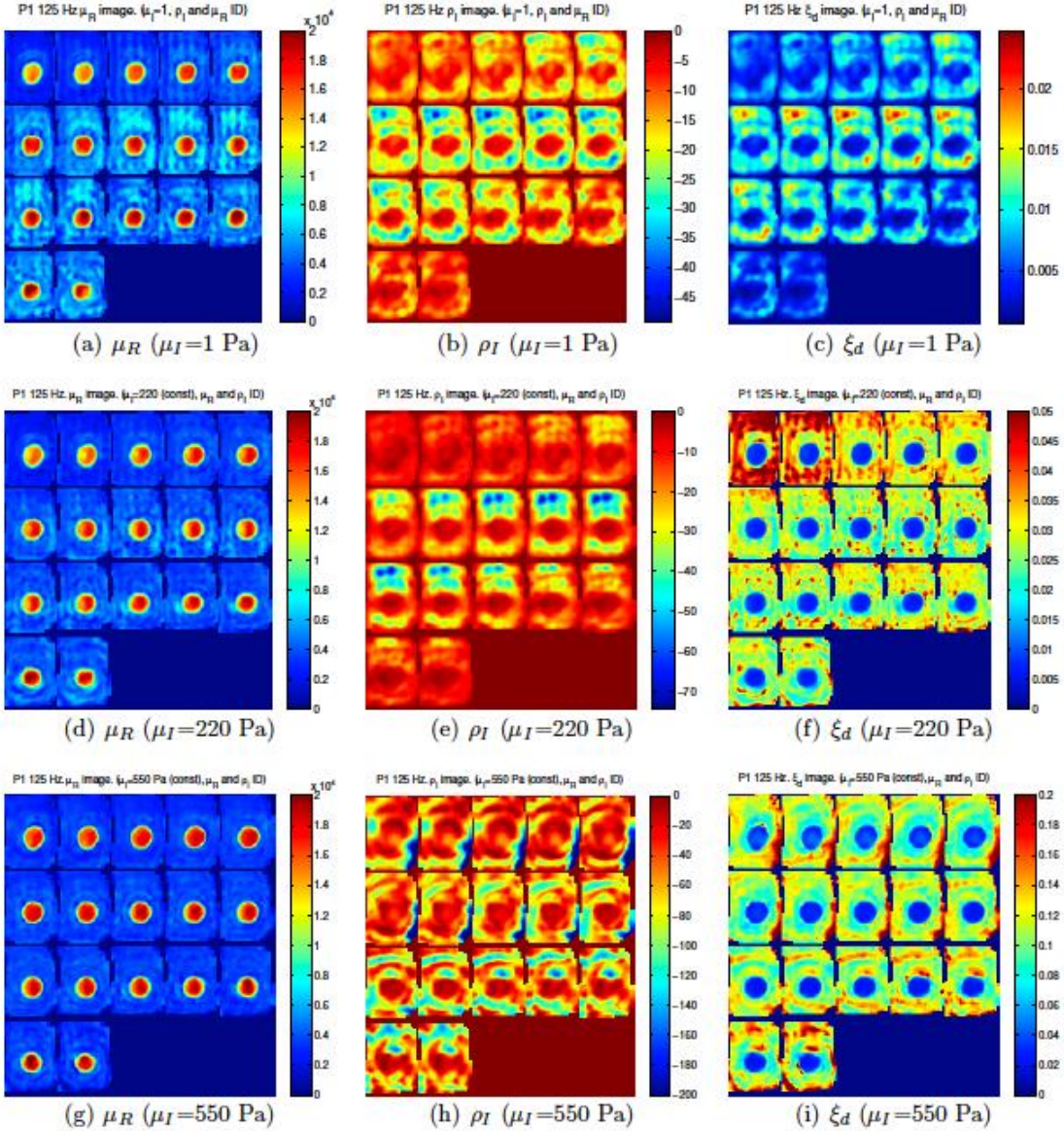

(a) μ_R (μ_I=1 Pa) (b) ρ_I (μ_I=1 Pa) (c) ξ_d (μ_I=1 Pa)

(d) μ_R (μ_I=220 Pa) (e) ρ_I (μ_I=220 Pa) (f) ξ_d (μ_I=220 Pa)

(g) μ_R (μ_I=550 Pa) (h) ρ_I (μ_I=550 Pa) (i) ξ_d (μ_I=550 Pa)

Parametric RD reconstructions

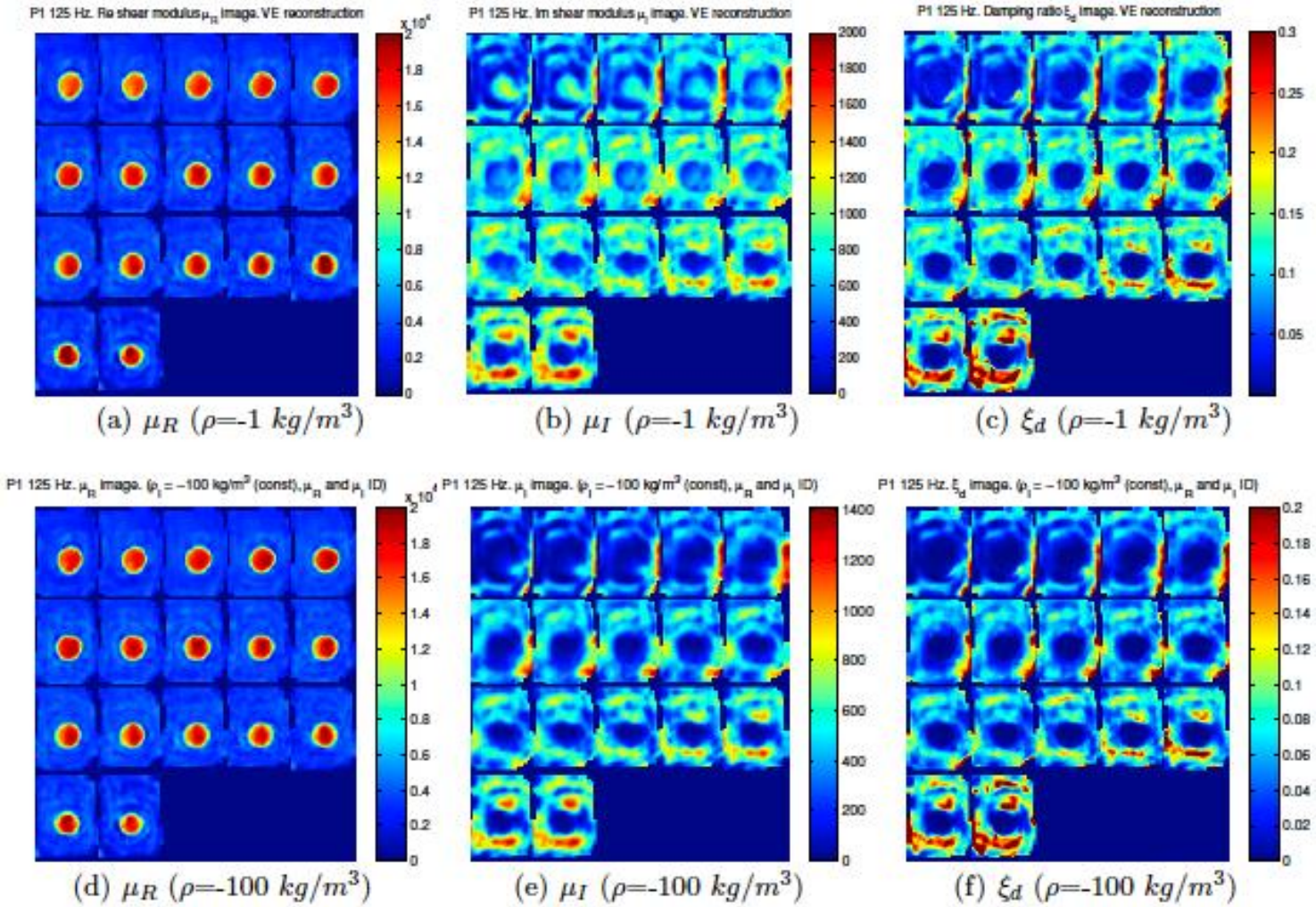

(a) μ_R (ρ=-1 kg/m^3) (b) μ_I (ρ=-1 kg/m^3) (c) ξ_d (ρ=-1 kg/m^3)

(d) μ_R (ρ=-100 kg/m^3) (e) μ_I (ρ=-100 kg/m^3) (f) ξ_d (ρ=-100 kg/m^3)

In vivo brain studies

Data acquisition

- 24 year old healthy volunteer at the University of Illinois Urbana-Champaign
- Actuation by speaker membrane connected to head cradle via long rod
- 50 Hz
- Performed using a 3T Allegra head-only scanner
- 3D motion encoding by a multishot spin echo (SE) sequence with bi-polar spiral motion encoding gradients (MEGs)

Data processing

- Undertaken using code developed by Van Houten and McGarry
- Employed High Performance Computing (HPC) Blue fern P575 at the University of Canterbury

In vivo brain RD MRE studies

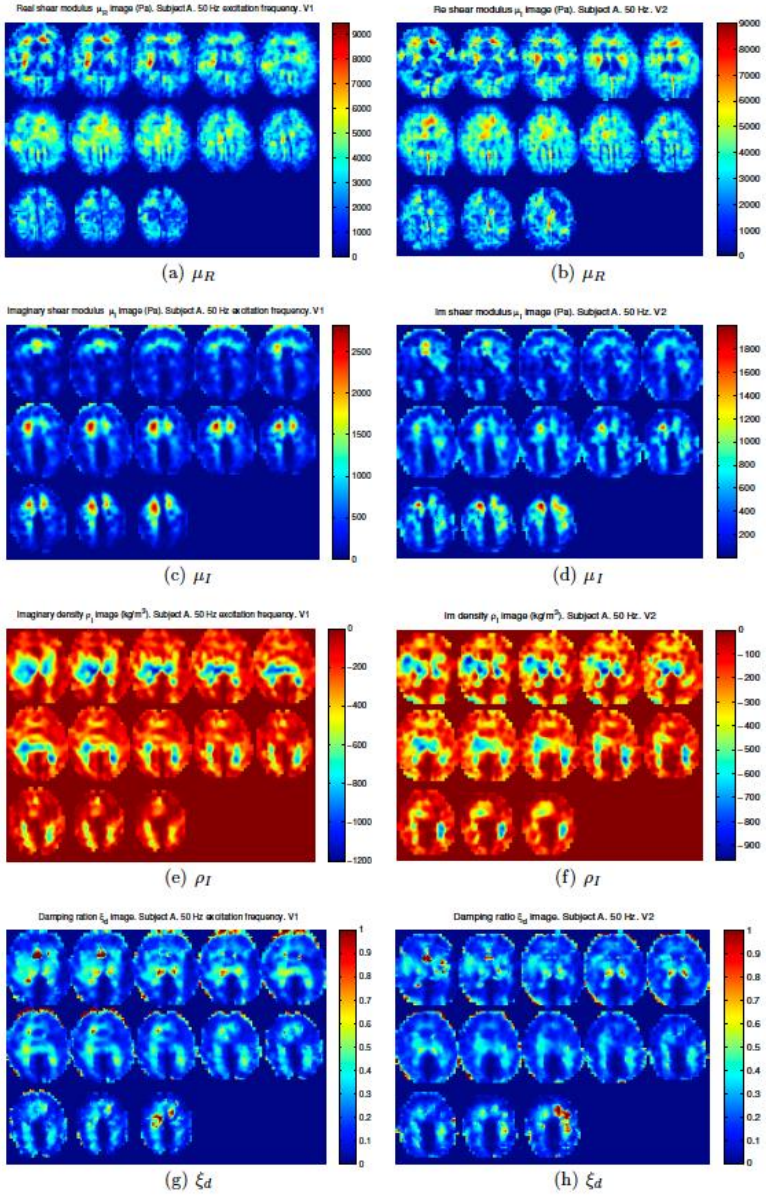

Simultaneous three-parameter single frequency RD reconstruction

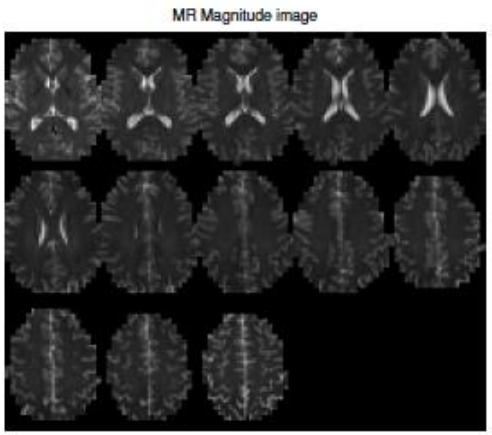

In vivo brain RD MRE studies

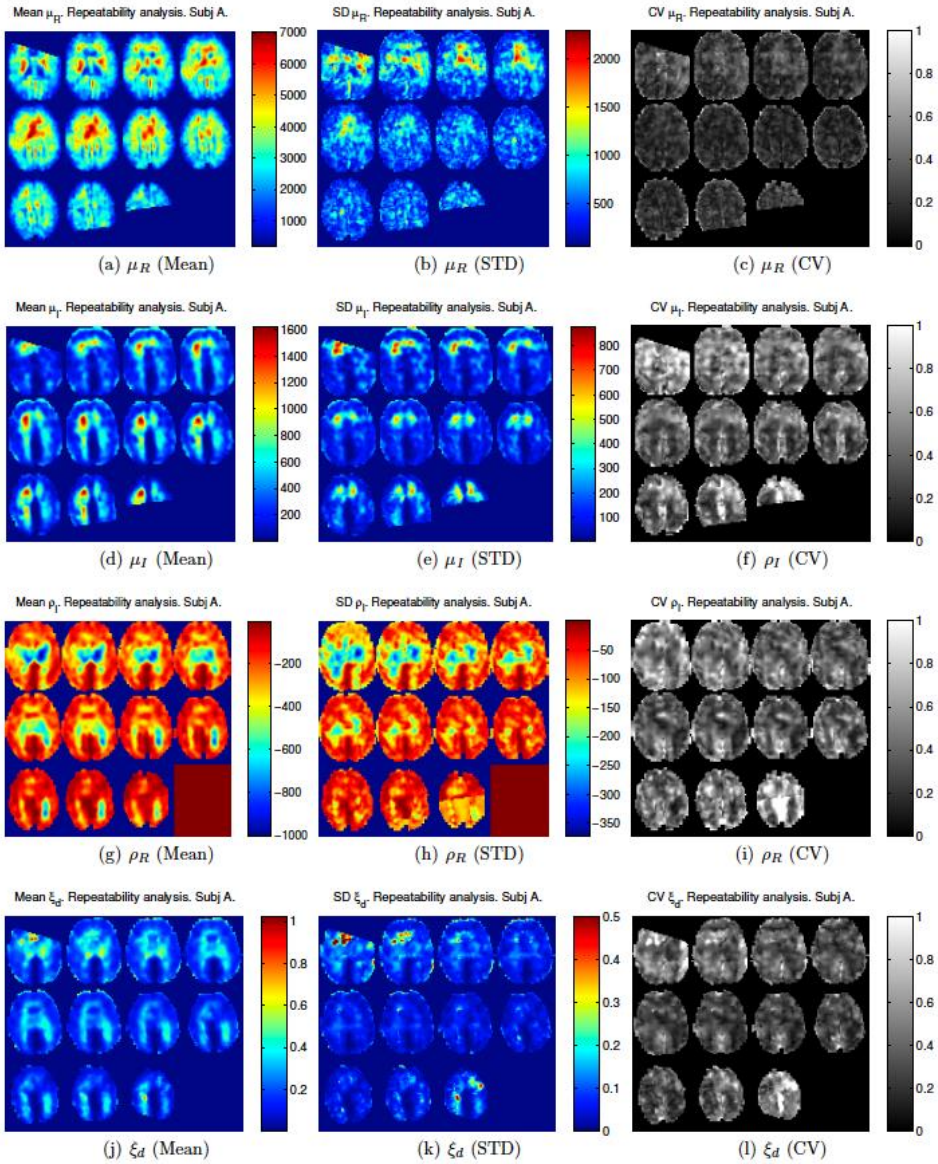

In vivo brain RD MRE studies

Table 10.1 ROI analysis of the in-vivo healthy brain

Parameter Units	OSS-SNR	μ_R (kPa)	μ_I (kPa)	ρ_I (kg/m^3)	ξ_d (%/100)
White matter					
Mean	**3.988**	**3.011**	**0.466**	**-320.608**	**0.250**
CV	0.209	0.038	0.171	-0.0494	0.061
Gray matter					
Mean	**4.967**	**2.193**	**0.305**	**-246.671**	**0.231**
CV	0.214	0.053	0.167	-0.0926	0.011

In vivo brain RD MRE studies

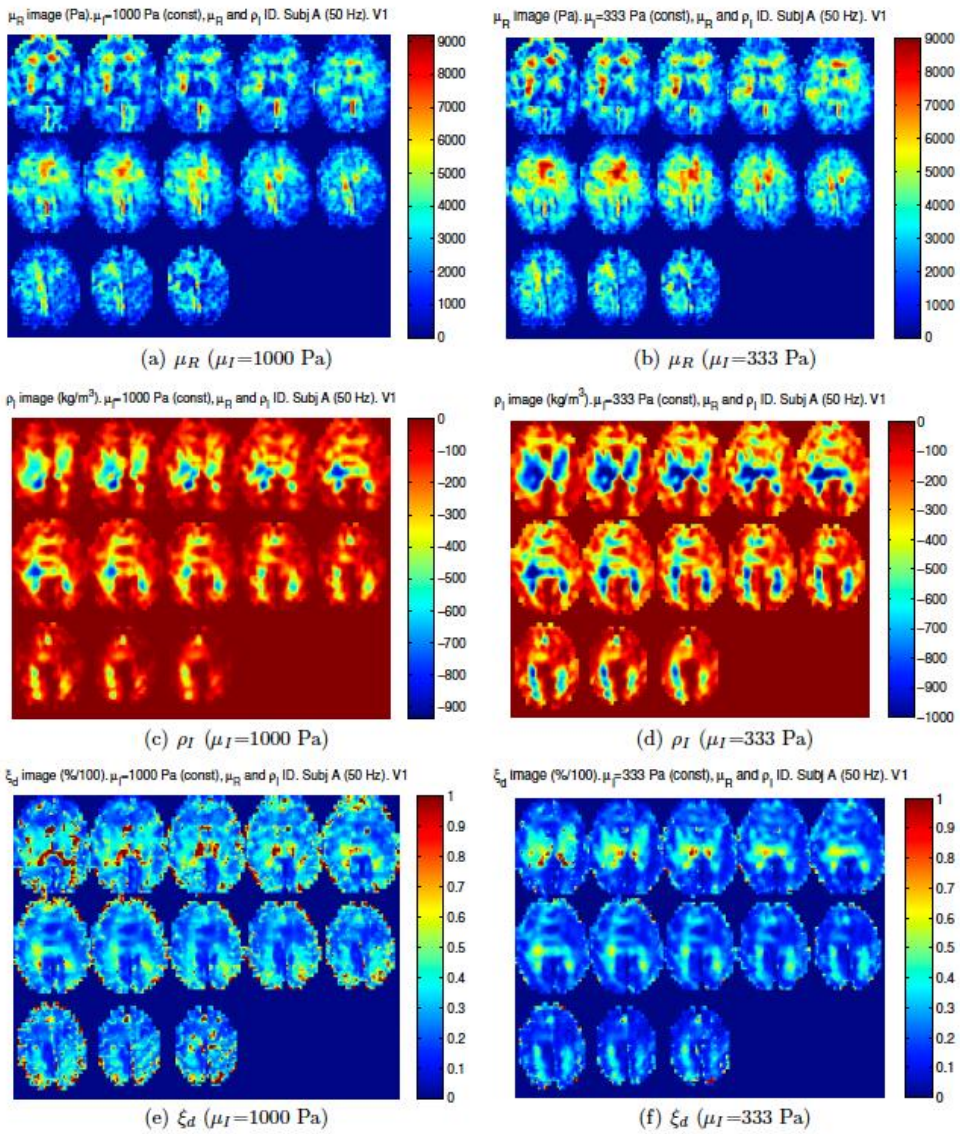

(a) μ_R (μ_I=1000 Pa) (b) μ_R (μ_I=333 Pa)

(c) ρ_I (μ_I=1000 Pa) (d) ρ_I (μ_I=333 Pa)

(e) ξ_d (μ_I=1000 Pa) (f) ξ_d (μ_I=333 Pa)

Parametric outcomes

- Utilising parametric methods, the structure of the brain is visible
- This may enable detection of occlusions
- The values of damping are still not unique and cannot be considered representative of the true state

Conclusions

Overall, this research has shown that while the Rayleigh damping model *may be* a suitable model for the mechanical properties of the brain, limitations in the quality of data are a barrier to clinical benefit.

Ultimately, this research is currently immature and cannot provide benefit at this stage.

We have shown that the model is effectively non-identifiable, but have also shown that it can be theoretically identified when multiple frequency data is used.

Parametric approaches can be used to elucidate some of the structures present and may be of some benefit if future studies can find suitable a-priori information or image manipulation strategies.

Acknowledgements

This work was supported by EU FP7 IRSES (FP7-PEOPLE-2012-IRSES) program, project title: eTime - Engineering Technology-based Innovation in Medicine, Grant No. 318943.

Acknowledgements

Thanks go to my co-authors: Andrii Petrov, Geoff Chase, Mathieu Sellier

Further thanks to Eli van Houten and Matt McGarry for access to computational codes and expertise

Questions?